

A MICROMACHINED THERMOELASTIC INCHWORM ACTUATOR

Ho Nam Kwon, Jong Hyun Lee, Sung Ho Jeong, Sun Kyu Lee

K-JIST, Gwangju, Korea

E-mail : jonghyun@kjist.ac.kr

Abstract

A new micromachined inchworm motor has been designed and fabricated for micro assembly applications. In order to implement inchworm motions, two thermoelastic actuators are contrived to have five-linkage mechanism with two-dimensional motions in tangential and normal directions. The thermoelastic actuators consist of two amplification bars and two coupling bars with four hinge springs. A forked tip, located on the apex of the linkage, is used to fit the teeth of shuttle mass for inchworm operation. The thermal expansion of the active bar generates the displacement of the actuator, which is then transformed into a bending of the active hinges to be finally amplified by the amplification bar. The inchworm actuator progressed by the designed steps of 5 μm and latched up by the teeth. The estimated driving force was 50 μN with less than 0.2 μm tolerance.

1. Introduction

For micro assembly applications, an actuator should be able to translate a small workpiece with an appropriate chucking force not to drop the workpiece during operation. The micro chuck needs to have a gripping force greater than tens of μN to grip the workpiece and a stroke longer than tens of μm [1]. In order to realize a high precision and long stroke translation system, electrostatic driven comb drivers and inchworm motors were suggested as driving actuators [2][3][4]. Unfortunately, the driving force from

electrostatic actuator tends to be small, and it is necessary to either apply a high voltage to attain a large displacement. Meanwhile, a thermoelastic actuator was fabricated for considerably large force and long stroke applications [5]. However, this actuator still provides insufficient force and non-rectilinear motion.

In this work, a new micromachined inchworm motor has been designed, fabricated and characterized for micro assembly applications of high force and long stroke.

2. Design of the inchworm motor

The proposed inchworm motor consists of one shuttle mass suspended by four leaf springs and a pair of five-linkage actuators, as shown in Fig. 1(a) [6]. The five-linkage mechanism provides the motion of two degree of freedom using two active hinge points, two shoulder hinges, and one neck hinge. And additional neck hinge and the forked tip (end effector) were added to grip the shuttle mass. Because the link between two neck hinges is so short that it works as one hinge point, we can consider the proposed mechanism as a five-linkage. When an input voltage is applied to two electrical pads of the actuator, induced electric current flow raises the temperature of the active bar and two active hinges, and t amplified displacement can be obtained from the thermal expansion of active bars and rotation of the amplification bar.

To secure the actuation without slipping, we contrived the teeth structure at the interface between the shuttle mass and the forked tip.

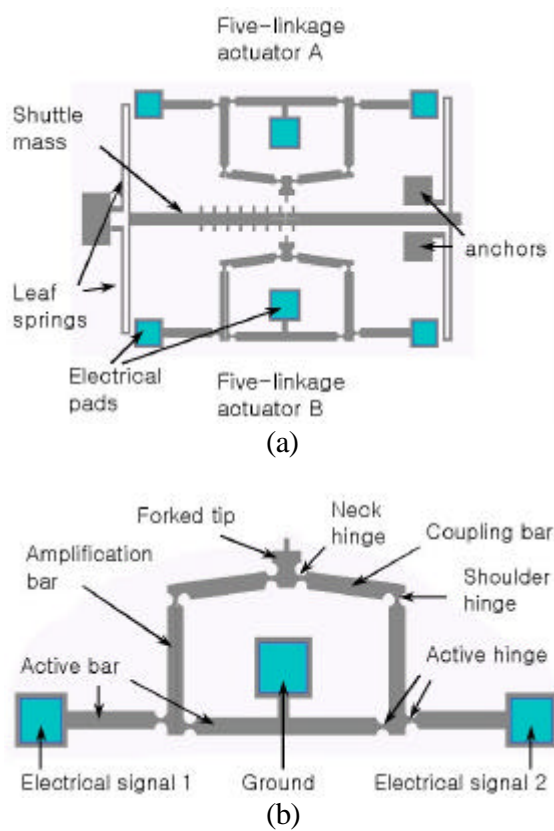


Figure 1. Schematics of proposed inchworm motor with thermoelastic actuators, (a) overall view of the inchworm motor, and (b) five-linkage mechanism for 2-dim actuation.

If the two amplification bars rotate in-phase, the forked tip will either move leftward/rightward with/without the shuttle mass or return to its initial state, as shown in Fig. 2(b), (d) and (f), respectively. On the contrary, if the two amplification bars rotate out-of-phase, the forked tip moves either inward for fitting or outward for releasing the shuttle mass, as shown in Fig. 2(c) and (e), respectively.

One pair of actuators is capable of four kinds of motion, such as fitting a forked tip, rectilinear driving of shuttle mass, releasing the shuttle mass, and returning to its initial state, as illustrated in Fig. 3. In this way, one cycle of stepping motion enables the inchworm motor to have a large stroke by

accumulating many stepping movements. In addition, the teeth may reduce power consumption by latch-up after driving.

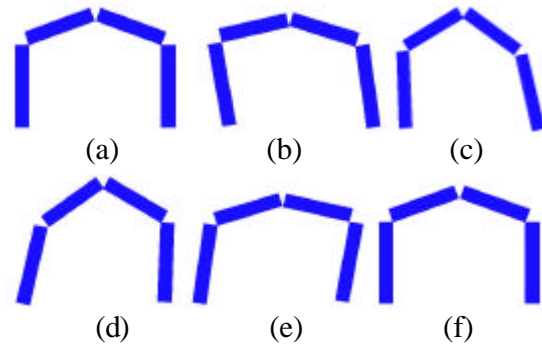


Figure 2. Unit steps of the linkage mechanism, (a) initial state, (b) leftward motion, (c) closing motion for fitting, (d) rightward motion for driving, (e) opening motion for releasing, and (f) in-phase leftward motion for returning to initial state.

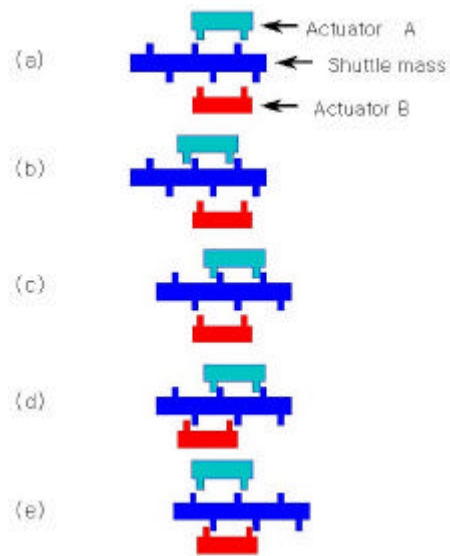


Figure 3. Inch-worm actuation with forked tips, (a) initial state, (b) fitting of the forked tip into the shuttle mass by actuator A, (c) rightward driving by actuator A, (d) fitting by actuator B, and (e) extracting and returning to initial state by actuator A, and rightward driving by actuator B.

3. Theoretical analysis

3.1. Operational schemes

In order to utilize the proposed thermoelastic actuator for inchworm motors, the required trajectory was investigated for one cycle of operation, as shown in Fig. 4. The trajectory consists of 4 unit steps, such as 1) extrusion for fitting, 2) driving for transportation, 3) retraction for release, and 4) contraction to initial location. Fig. 4 also shows the required voltages for right and left linkage actuators to perform inchworm motion according to the cyclic sequence. We can see from the diagram that the required strokes are about 5 μm and 2 μm in tangential and normal directions, respectively. This mechanism is very useful for the microsystem to meet the requirements from large force applications or switching devices with discrete displacement.

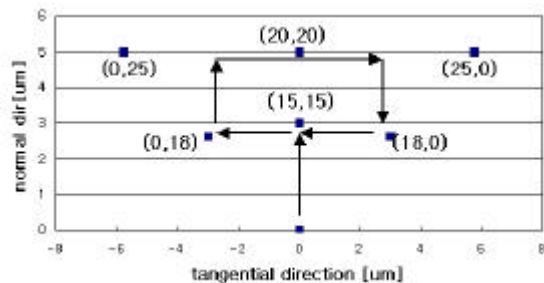


Figure 4. Estimated trajectory of one cyclic motion for inchworm motors based on FEA.

3.2. Stiffness of the actuator

The stiffness at the top of the forked tip is used to estimate the maximum force that the thermoelastic actuator can exert to the shuttle mass. The resultant stiffness of the forked tip can be estimated to be 286 N/m from FEA. We also found that the actuator can generate a driving force over 50 μN with a placement tolerance of 0.2 μm .

4. Device fabrication

We fabricated the proposed thermoelastic actuators using SOI (silicon-on-insulator) wafers. The minimum feature size was 2 μm , which corresponds to the width of one tooth. The device layer of 40 μm in thickness was micromachined with DRIE (Deep Reactive Ion Etching) process and was doped with phosphorus to control its electrical resistance. The sacrificial oxide layer was removed using HF GPE (Gas-Phase etching) process with no virtual stiction of microstructures.

5. Experimental characterization

Fig. 5 shows that the response time of the fabricated actuator is about 4 msec by 90% of rising time criterion from step response. Dynamic characteristics of the fabricated micro inchworm motor were experimentally investigated to evaluate its performance. First of all, the upper actuator A drove the shuttle mass one step, and the counterpart actuator B drove another step, next the actuator A drove one more step and latched up the shuttle mass as shown in Fig 6(a),(b),(c) respectively. By three steps of the inchworm motion, the accumulated displacement was 15 μm as shown in Fig 6(d).

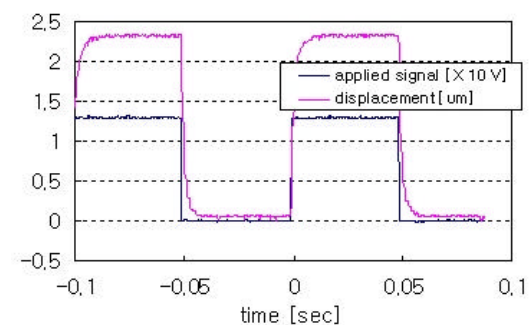


Figure 5. Step response of a thermoelastic actuator with a linkage mechanism

Using the fabricated micro inchworm motors, the gripping of a workpiece like an optical fiber is under investigation as shown in Fig. 7.

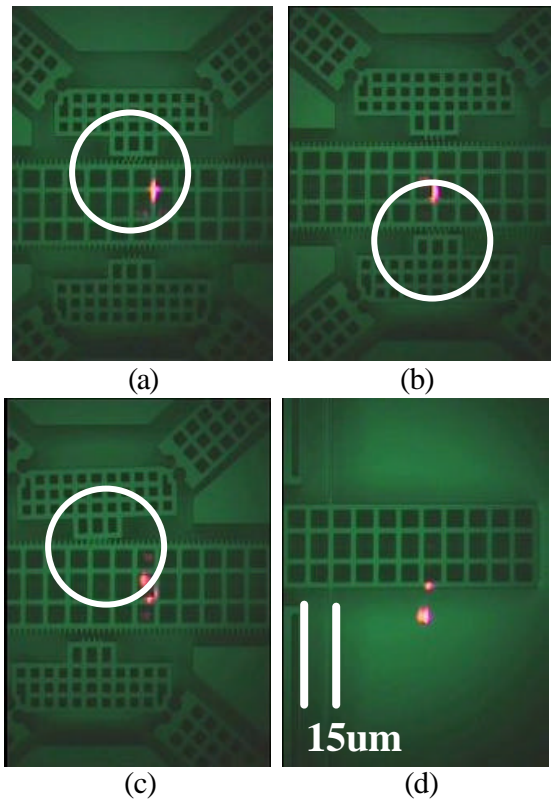


Figure 6. Video images of the inchworm motions, (a) 1st step by top actuator, (b) 2nd step by bottom actuator, (c) 3rd step and latch up by the top actuator, and (d) accumulated stroke of 3 steps. Notice the difference between the locations of the end effector in (a) and (c).

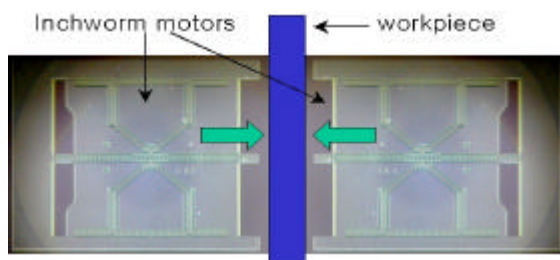


Figure 7. Schematic of gripping a workpiece with one pair of the inchworm motors.

6. Conclusion

A micromachined thermoelastic inchworm motor was fabricated and characterized SOI wafer with the structural layer 40 um thickness was used to fabricate the proposed inchworm motors, and the inchworm motion was experimentally investigated by the cyclic motion. The motor is applicable to the micro precision stage for micro assembly or switching devices. As a further study, gripping a workpiece with the motors is under investigation using the fabricated actuators and the control circuit.

Acknowledgement

This work was supported by BK21 project. The authors would like to thank ETRI and LG Elite for their technical supports in connection with fabrication of the device presented in this paper.

References

- [1] K. Tsuchiya, M. Nakao, T. Okusa, Y. Hatamura, and K. Matsumoto, SPIE MMF, pp.147-156, Jan. 1997.
- [2] W. C. Tang, Tu-Cuong, H. Nguyen, and R. T. Howe, Proc. MEMS, pp.53-59, Jan. 1989.
- [3] N. R. Tas, A. H. Sonnenberg, A. F. M. Sander, and M. C. Elwenspoke, Proc. MEMS, pp.215-220, Jan. 1997.
- [4] R. Yeh, S. Hollar, and K. S. J. Pister, Proc. MEMS, pp. 260-264, Jan. 2001.
- [5] E. S. Kolesar, P. B. Allen, J. T. Howard, J. M. Wilken, and N. C. Boydston, J. Vac. Sci. Technol. A, 17(4), pp.2257-2263, Jul/Aug. 1999.
- [6] H. N. Kwon, J. H. Lee, S. H. Jeong, S. K. Lee, W. I. Jang, and C. A. Choi, 32nd ISR, pp. 796-801, Apr. 2001.